ELSEVIER

Biochimica et Biophysica Acta 1192 (1994) 253–262

BBA Biochimica et Biophysica Acta

Interactions of liposome bilayers composed of 1,2-diacyl-3-succinylglycerol with protons and divalent cations

Ana M. Tari [a,1], Nola Fuller [b], Lawrence T. Boni [c], David Collins [a,2], Peter Rand [b], Leaf Huang [a,*]

[a] *Department of Biochemistry, University of Tennessee, Knoxville, TN 37996-0840, USA*
[b] *Department of Biological Sciences, Brock University, St. Catharines, Ontario, L2S 3A1, Canada*
[c] *The Liposome Company, Inc., 1 Research Way, Princeton, NJ 08540, USA*

(Received 30 September 1993)

Abstract

Bilayer liposomes were prepared by using pure DOSG (1,2-dioleoyl-3-succinylglycerol) or DPSG (1,2-dipalmitoyl-3-succinylglycerol) at pH 7.4 or above. These liposomes undergo destabilization upon incubation with acid. When calcein was used as an entrapped aqueous marker, half maximal content leakage was observed between pH 5.8–6.3. Differential scanning calorimetry showed that at pH 7.4, the chain-melting temperature (T_m) of DPSG was 60.4°C, and increased with decreasing pH (T_m = 57.0°C and 62.7°C at pH 8.9 and 6.7, respectively). Below pH 6.7, extensive phase separation occurred as the major chain melting peak split into three peaks. These three peaks coalesced into one peak below pH 5. Freeze fracture electron micrographs of DOSG liposomes at pH 4 showed the formation of non-bilayer as well as hexagonal phase structures. The effects of divalent cations, such as Ca^{2+} and Mg^{2+}, on the destabilization of DASG bilayers have also been studied. Differential scanning calorimetry studies of bilayers composed of DPSG showed that both Ca^{2+} and Mg^{2+} could increase the T_m of DPSG with increasing concentrations. However, under identical conditions Mg^{2+} was more effective than Ca^{2+} in increasing the T_m of DPSG. X-ray diffraction indicated that both Ca^{2+} and Mg^{2+} could induce DPSG bilayers to undergo a complete lamellar to hexagonal phase transition. There was a size-dependency on the plasma stability of DOSG liposomes. DOSG liposomes that were smaller in size were more stable in plasma than the larger ones. After incubation with plasma, DOSG liposomes became less acid-sensitive. DOSG immunoliposomes entrapping diphtheria toxin A chain were used as a model for cytoplasmic delivery of the novel pH-sensitive liposomes. The delivery activity was comparable to that of the conventional pH-sensitive liposomes containing unsaturated phosphatidylethanolamine. Our data indicate that the mechanism of liposome destabilization involves extensive bilayer phase separation as well as the formation of non-bilayer structures.

Key words: Acid-sensitive liposome; Diacylsuccinylglycerol; Divalent cation; Phase separation; Non-bilayer phase; Drug delivery

1. Introduction

Cytoplasmic delivery of bioactive molecules is an important goal of the targeted drug delivery. This is particularly the case for macromolecules such as enzymes, antibodies and nucleic acids because they do not easily penetrate the cellular membranes. Fusogenic, pH-sensitive liposomes have been developed for this purpose because of their enhanced cytoplasmic delivery activity [1]. This class of liposomes is stable

* Corresponding author.
[1] Present address: Department of Clinical Investigations, Box 60, M.D. Anderson Cancer Center, Houston, TX 77030, USA.
[2] Present address: AmGen Corporation, 1840 DeHavilland Drive, Thousand Oaks, CA 91320, USA.

Abbreviations: DASG, 1,2-diacyl-3-succinylglycerol; DOC, deoxycholate; DOPE, dioleoyl-PE; DOSG, 1,2-dioleoyl-3-succinylglycerol; DPSG, 1,2-dipalmitoyl-3-succinylglycerol; DTA, A-chain of diphtheria toxin; Hepes, *N*-2-hydroxyethylpiperazine-*N'*-2-ethanesulfonic acid; Hepps, *N*-2-hydroxyethylpiperazine-*N'*-3-propanesulfonic acid; MLV, multilamellar vesicles; PBS, phosphate-buffered saline (137 mM NaCl, 2.7 mM; KCl, 1.5 mM KH_2PO_4 and 1 mM Na_2HPO_4); PE, phosphatidylethanolamine; Pipes, piperazine-*N*,*N'*-bis(2-ethanesulfonic acid); REV, reverse-phase evaporation vesicles; SUV, small unilamellar vesicles.

SSDI 0005-2736(94)00080-9

and non-fusogenic at neutral pH but becomes destabilized and fusogenic at a mildly acidic pH, such as pH 5–6 [2–4]. pH-sensitive liposomes, similar to all other liposomes types, are internalized by cells via an endocytic mechanism [5,6]. These liposomes release their entrapped contents into the cytoplasm when they encounter the acidic environment in the endocytic compartment and destabilize [1–4,7]. Antitumor drugs [8], fluorescent dyes [9], toxin [7] and DNA [10,11] have been successfully delivered by this class of liposomes.

The basic design of pH-sensitive liposomes takes advantage of the high tendency of unsaturated phosphatidylethanolamine (PE) to form the reverse hexagonal phase at physiological temperature, pH and ionic strength [12]. Stable bilayer liposomes, however, can be prepared by mixing the unsaturated PE with a weakly acidic amphiphile such as fatty acids [4,13], fatty acyl amino acid [2], cholesterol hemisuccinate [3] and acid conjugates of PE [14]. DASG was first described by Leventis et al. [15] as a double-chain acidic amphiphile which can stabilize the Lα phase of unsaturated PE. When DASG is protonated at acidic pH, a rapid destabilization of the PE bilayer occurs primarily due to a phase transition to the non-bilayer phases [3,4,15]. It has been shown by us that liposomes composed of DOPE and DASG are an effective cytoplasmic delivery vehicle for DTA [16]. Furthermore, the delivery event takes place at 20–25 min after the liposomes are endocytosed, indicating that the site of cytoplasmic release is the late endosome or lysosome compartment [17].

Ca^{2+} and Mg^{2+} are important components of biological fluids and tissure culture media. These divalent cations have also been shown to destabilize liposomes containing anionic lipids, such as phosphatidylserine [18–21], phosphatidic acid [22] and cardiolipin [23–25]. Furthermore, acid-sensitive liposomes are often sensitive to divalent cations [26,27]. These cations may play an important role in augmenting the membrane fusion and destabilization events in the endosomes.

We describe here that stable bilayer liposomes can be prepared with an aqueous dispersion of pure DASG, i.e., no unsaturated PE is required. Stabilities of these liposomes at different pH values have been studied with liposomes of the dioleoyl form of DASG by the entrapped content leakage. The thermal phase transition of DPSG is also studied with differential scanning calorimetry. These studies have shed light on the mechanism of the acid-induced bilayer destabilization of DASG. Since DASG is an anionic lipid, Ca^{2+} and Mg^{2+} could also affect the stability of liposomes composed of DASG. We have used differential scanning calorimetry and X-ray diffraction to examine the stability of DASG bilayers in the presence of divalent cations. Furthermore, we have shown that DOSG liposomes can deliver a protein toxin to target cells and have compared this cytoplasmic delivery activity with that of the conventional pH-sensitive liposomes composed of primarily unsaturated PE. Preliminary accounts of the project have been reported previously [28,29].

2. Materials and methods

2.1. Materials

DOSG and DPSG were purchased from Avanti Polar Lipids (Birmingham, AL). The purity of the lipids was confirmed by thin-layer chromatography using hexane/ethylether/methanol/acetic acid (70:30:5:1, v/v) as a developing solvent system. Other lipids were also purchased from Avanti. Calcein and DOC were purchased from Sigma (St. Louis, MO) and used without further purification. [^{3}H]Leucine was purchased from New England Nuclear (Boston, MA). Ricin was isolated from castor beans by the method of Nicholson and Blaustein [30]. Anti-H2K^k antibody (11–4.1) was purified, labeled with ^{125}I, and derivatized with *N*-hydroxysuccinimide ester of palmitic acid, as described by Huang et al. [31]. DTA was prepared from intact toxin by the method of Gill and Dinius [32], and labeled with ^{131}I by the iodobead methods according to the manufacturer's protocol (Pierce, Rockford, IL).

2.2. Liposome preparation

Liposomes were prepared by two different methods. Method 1 involved the preparation of SUV. A thin film of solvent-free lipids was vacuum desiccated for at least 30 min. A trace amount of hexadecyl [^{3}H]cholestanyl ether was added to the lipids to monitor lipid concentration. The lipids were suspended in PBS, containing 1 mM EDTA with or without 50 mM calcein, at a final concentration of 10 μmol/ml for 2–4 h before a 20-min sonication in a bath sonicator (Laboratory Supplies, Hicksville, NY). The pH of the suspension was maintained between 7.8–8.2 by adding 1 M NaOH. The sonicate was then incubated overnight for equilibration at room temperature. Untrapped calcein was removed by gel filtration of the liposome suspension on a Bio-Gel A-0.5 m column. Calcein-containing liposomes were further passed over a Sepharose 4B column to obtain different pools of size of SUV. The size of liposomes was measured by dynamic laser light scattering using a Coulter N4SD instrument.

Method 2 involved the preparation of reverse-phase evaporation vesicles (REV) [33]. Solvent-free DOSG was vacuum desiccated and suspended in PBS containing 0.2 mg/ml DTA. A trace amount of hexadecyl [^{3}H]cholestanyl ether was added as a radioactive lipid marker. The lipid suspension was sonicated at room

temperature for 10 min with a bath sonicator. The pH of the sonicate was maintained between pH 8.0–8.5 by adding 1 M NaOH. Diethyl ether was then added to the aqueous phase (3:1, v/v). The mixture was sonicated for 30 sec to form a stable emulsion which was rotary evaporated at room temperature until all of the organic phase was removed. The resulting REV were incubated in a fume hood for 1 h to remove any residual organic solvent. PBS was added to the REV suspension to bring the final lipid concentration to 10 mM. Palmitoyl antibody was then added to the liposomes with a lipid-to-protein ratio of 10:1 (w/w) to allow the incorporation of antibody into liposomes [7]. Untrapped DTA was separated from liposomes by gel filtration using a Bio-Gel A-0.5 m column. The liposomes were then extruded through a 0.2 μm polycarbonate filter (Nucleopore) to obtain size uniformity.

2.3. Pretreatment of liposomes with plasma

250 μl of calcein-containing SUV were mixed with the same volume of plasma and incubated for 1 h at 37°C before passing through a Bio-Gel A-1.5 m column to separate free plasma components from liposomes. The liposomal fractions were pooled and acid-sensitivity of liposomes was then determined.

2.4. Content leakage of liposomes

Calcein-containing SUV was prepared as described above. A LS-5 Perkin-Elmer spectrophotometer was used for the fluorescence assay. The excitation and emission wavelengths were 490 nm and 520 nm, respectively. The excitation and emission slit widths were 5 nm and 3 nm, respectively. 5 μl of liposomes were added to a cuvette containing 2 ml of PBS (pH 7.4). After the relative fluorescence was measured, 0–20 μl of 0.5 N HCl was added to achieve the desired pH. After continuous stirring at room temperature for 2 min, appropriate amounts of 0.5 M NaOH were added to bring the pH back up to 7.4. The relative fluorescence was again measured. DOC was then added, at a final concentration of 0.15%, to disrupt the liposomes. Percent release was calculated from the following formula:

$$\% \text{ Release} = ((F - F_o)/(F_t - F_o)) \times 100$$

where F_o = fluorescence intensity of liposomes before acidification, F = fluorescence intensity after acid incubation and F_t = fluorescence intensity after DOC addition.

2.5. Stability of liposomes in plasma

Calcein-containing SUV, ranging from 60–260 nm in diameter, was used to determine the stability of liposomes in plasma. 50 μl of liposomes containing 50 nmol of lipid were added to 450 μl of serum prewarmed to 37°C. 10 μl of the mixture were used for the fluorescence measurement at different incubation time-points. DOC was then added. Percent release of liposomal calcein was calculated as above, except F_o = fluorescence intensity of liposomes in PBS at time zero, F = fluorescence intensity at different time-points and F_t = fluorescence intensity after DOC addition.

2.6. Freeze-fracture electron microscopy

A thin film of DOSG lipids was suspended at 1 μmol/ml in 20 mM Pipes or 20 mM succinic acid buffer containing 1 mM EDTA. The lipids were kept initially at pH 7.4 and extruded through 0.2 μm polycarbonate filters. The pH of the liposome suspension was then lowered to pH 6.0 or 4.0 by adding 1 M HCl. The liposomes were incubated at the desired pH for at least 2 h before viewed with freeze fracture electron microscopy. The freeze fracture procedure was done as described [26]. The replicas were viewed on a Philips 300 electron microscope at magnifications of 7000 to 27000.

2.7. X-ray diffraction

The hydrated lipids were mounted into X-ray sample holders at the equilibrating temperature. Each sample was combined with some powdered teflon as an X-ray calibration standard and then sealed between mica windows 1 mm apart. X-ray diffraction was used to characterize the structures formed by the various lipid mixtures. The $CuK_{\alpha 1}$ line (λ = 1.540 Å) was isolated using a bent quartz crystal monochromator, and diffraction patterns were recorded photographically using Guinier X-ray cameras operating in vacuo. Temperature was controlled with thermoelectric elements to approximately $\pm$0.5°C.

A lamellar phase is characterized by a series of three to five X-ray spacings in the ratios of the unit cell dimension, d_{lam} of 1, 1/2, 1/3, 1/4, etc. A hexagonal phase is characterized by X-ray spacings bearing ratios to the dimension of the first order, d_{hex} of 1, $1/\sqrt{3}$, $1/\sqrt{4}$, $1/\sqrt{7}$, $1/\sqrt{9}$, $1/\sqrt{11}$, etc.

2.8. Differential scanning calorimetry

In the presence of acid

After vacuum desiccation, solvent-free lipids were suspended at 5 μmol/ml in one of these buffers: (i) 20 mM Pipes with 1 mM EDTA, (ii) 20 mM Hepes with 1 mM EDTA, (iii) 20 mM Hepps with 1 mM EDTA or (iv) 20 mM succinic acid with 1 mM EDTA. The initial pH of all buffers was pH 7.4. DOSG and DPSG were

hydrated, and vortexed occasionally, for 3 h at room temperature and 67°C, respectively. Various amounts of 1 M HCl or 1 M NaOH were added to the lipid mixture to achieve the desired pH. Lipids were vortexed and further incubated at the appropriate temperature and desired pH for an additional h before incubation at room temperature for overnight equilibration.

In the presence of divalent cations

After vacuum dessication, solvent free lipids were suspended at 5 μmol/ml in 20 mM Pipes buffer (pH 7.4). DPSG was hydrated and vortexed occasionally for 2 h at 67°C. Various amounts of $CaCl_2$ or $MgCl_2$ were then added to the lipid mixture. To some lipid samples, various amounts of 1 M HCl were also added so that the final pH of the mixture was 6.8. Lipids were vortexed and further incubated for 2 additional h at 67°C before incubation at room temperature for overnight equilibration.

The equilibrated lipids were loaded into a Microcal MC-2 scanning calorimeter (Amherst, MA) and scanned from 20 to 80°C at a scan rate of 30°C/h. The excess heat capacity was recorded as a function of temperature. The peak transition temperature was determined by an IBM PC computer interfaced with the instrument. The pH of the samples was measured before and after the scan. The variation of pH of the samples was always within 0.05 pH unit. The samples were scanned multiple times to obtain reproducible thermograms which reflect the equilibrium state of the samples.

2.9. Cytotoxicity assay

The cytotoxicity assay was done as described previously [7], except after a 6 h [^{3}H]leucine incubation, cells were washed, trypsinized and harvested with a PHD cell harvester (Cambridge Technology). The filter remnants were processed for scintillation counting as described [7]. All experiments were done in five duplicates.

3. Results

3.1. Destabilization of DASG bilayers induced by acid

Entrapped content leakage

When DOSG vesicles were sonicated in the presence of 50 mM calcein (pH 7.4), and chromatographed on Bio-Gel A-0.5 m to remove unentrapped calcein, it was found that the vesicles could entrap calcein with a fluorescence quenching of 71–78% which indicates that the calcein concentration in the vesicles was approximately 50 mM [34]. The vesicles maintained this level

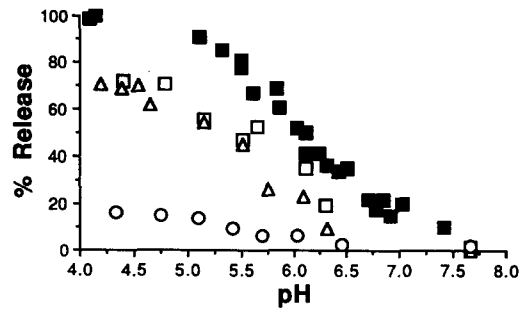

Fig. 1. Effect of acidification on calcein-release from SUV composed of DOSG. DOSG liposomes were 183±32 nm (□,■), 126±21 nm (△) and 62±8 nm (○) in diameter. Closed and open symbols represent DOSG liposomes before and after pretreatment with plasma, respectively.

of fluorescence quenching even after a prolonged storage in PBS (pH 7.4) at 4°C for 2–3 weeks. However, the entrapped calcein rapidly leaked out if the medium pH was lowered by adding acid (Fig. 1, closed symbol). 50% of calcein release was observed at pH 5.8–6.3. Sonicated DPSG vesicles which were prepared by full hydration at 67°C could also entrap calcein with 72–75% fluorescence quenching. The release of calcein from DPSG vesicles at acidic pH was similar to that of the DOSG vesicles (data not shown).

Bilayer destabilization at acidic pH was also measured with a lipid mixing assay, using *N*-(7-nitrobenz-2-oxa-1,3-diazol-4-yl)-PE and *N*-(lissamine rhodamine B-sulfonyl)-PE [35]. Acid-induced lipid mixing of DOSG vesicles showed a maximal mixing at approximately 60% at pH < 5, with the half-maximal mixing at about pH 5.8 (data not shown).

Thermal phase transition of DPSG dispersions

The phase behavior of DASG dispersions prepared as MLV was studied by differential scanning calorimetry. No endo- or exo-thermic transitions could be detected for DOSG dispersions between 0 and 90°C at pH 7.4 or lower, indicating no thermal phase changes occurred with this lipid in the temperature range tested. Fig. 2 shows heating scans of DPSG dispersions equilibrated at different pH values. At pH 7.4, two endothermic peaks appeared, one at 43.3°C and another at 60.4°C. In a separate experiment, using a trace amount of diphenylhexatriene incorporated into DPSG dispersion, the transition at 60.4°C was accompanied with a large decrease in the fluorescence polarization of the incorporated diphenylhexatriene (data not shown), indicating that this transition was the chain-melting transition. This result also implies that the transition at 42.3°C is a pretransition.

Enthalpies of the transitions are listed in Table 1. At lower pH values, there was a progressive increase of the transition temperature of the chain-melting peak (Fig. 2). For example, the main transition at pH 6.7

occurred at 62.7°C, approximately 2.3°C above the chain-melting temperature at pH 7.4. Below pH 6.7 the main transition split into 3 peaks. For instance, at pH 6.5, only one of those peaks remained at 62.7°C (Fig. 2) while the other two peaks appeared at 61.3°C and 63.3°C. This evidence of phase separation could also be observed at other acidic pH values. Splitting of the chain-melting transition peak into 3 peaks did not involve a change of the total transition enthalpy. At pH 7.4, $\Delta H = 7.1$ kcal/mol. At acidic pH values, the average sum of $\Delta H = 7.4$ kcal/mol. This phase separation event is likely the result of different DPSG domains which experience different degrees of protonation. Further decreasing the pH to 5.4, the peak at the lowest temperature (~ 59°C) became the dominant peak. The sum of ΔH still remained relatively constant. Thus, the lower temperature peak had increased its ΔH at the expense of the other two peaks. At even more acidic pH values, e.g., pH 4.6, only one peak (at 60.1°C) was observed; indicating that only a single dominant structure existed at this condition.

At pH 7.4 or above, the pre-transition peak was rather difficult to detect since it would not readily appear unless the DPSG dispersions had been equilibrated at room temperature for at least 39 h before scanning. At acidic pH values (< pH 6.8) the pre-transition peak could be readily observed.

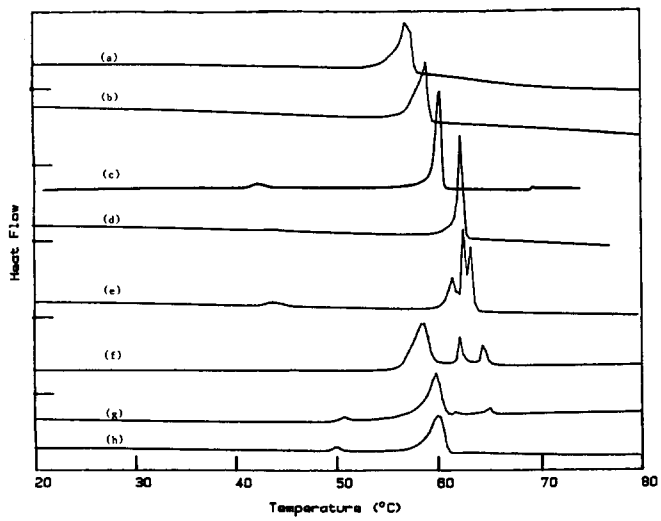

Fig. 2. Representative differential scanning calorimetry scans of DPSG dispersions at (a) pH 8.9, (b) 8.2, (c) 7.4, (d) 6.8, (e) 6.5, (f) 5.4, (g) 5.0 and (h) 4.6.

Freeze-fracture electron microscopy of DOSG liposomes

The polymorphic phase behavior of DOSG liposomes at different pH was also studied by freeze fracture electron microscopy. As shown in Fig. 3A, DOSG liposomes at pH 7.4 formed unilamellar vesicles of approximately 0.2 μm in diameter. Small aggregates of vesicles were sometimes noted. Under acidic conditions, DOSG liposomes were found to fuse (Fig. 3B–D). This fusion product exhibited morphological characteristics of non-bilayer phases. In certain specimens, striations resembling hexagonal phase tubes (Fig. 3B and C) and cross-fractures of tubes (Fig. 3D) were found along with the non-bilayer phases. However, hexagonal phase was not the predominant structure. The aggregation and fusion was more extensive at pH 4.0 as compared to pH 6.0. The structures at pH 4.0 also appeared to be more tightly packed than at pH 6.0.

Table 1
DSC data of T_p, T_m and ΔH of DPSG dispersions at different pH values [a]

pH	T_p (°C)		T_m (°C)			ΔH (kcal/mol)	
8.9	–		57.0 ± 0.1			7.6 ± 0.2	
8.4	–		58.6 ± 0.1			7.3 ± 0.2	
8.2	–		58.1 ± 0			7.6 ± 0.2	
8.0	–		59.4 ± 0.1			6.7 ± 0.1	
7.6	–		59.9 ± 0.1			6.3 ± 0.7	
7.4	42.3 ± 0		60.4 ± 0.1			7.1 ± 0.3	
7.2	–		61.3 ± 0.1			6.4 ± 0.2	
7.0	–		61.8 ± 0.1			6.2 ± 0.2	
6.8	43.7		62.4 ± 0			6.7 ± 0.1	
6.7	44.1 ± 0.4		62.7 ± 0			7.4 ± 0.1	
6.5	44.1 ± 0.1	61.3 ± 0.2	62.7 ± 0	63.3 ± 0.1	2.3 ± 0.3	3.5 ± 0.4	1.4 ± 0.1
6.3	44.2	59.5 ± 0.1	62.5 ± 0.1	63.8 ± 0.1	1.3 ± 0.4	2.7 ± 0.1	1.7 ± 0.3
6.1	44.4 ± 0.1	58.2 ± 0	62.5 ± 0.1	64.2 ± 0.1	2.3 ± 0.1	4.0 ± 0.1	1.4 ± 0.8
5.7	44.3 ± 0	58.7 ± 0	62.3 ± 0	63.9 ± 0.1	3.4 ± 0.4	1.3 ± 0.2	0.9 ± 0.6
5.4	45.1 ± 0.3	58.5 ± 0.2	62.1 ± 0.2	64.4 ± 0.1	7.4 ± 0.4	1.1 ± 0.4	0.9 ± 0.2
5.2	45.5 ± 0.3	59.2 ± 0.2	61.9 ± 0.1	64.6 ± 0	8.4 ± 0.6	0.2 ± 0	0.2 ± 0
5.0	50.7 ± 0.2	59.1 ± 0.1	61.2 ± 0.1	64.5 ± 0.1	7.3 ± 0.5	0.3 ± 0.1	0.3 ± 0.1
4.6	50.0	–	60.1 ± 0.2	–	–	6.9 ± 0.2	–

[a] ΔH values are matched with corresponding values of T_m. Data are average values of two independent experiments ± error.

3.2. Destabilization of DASG bilayers induced by divalent cations

Thermal phase transition of DPSG dispersions

Fig. 4 shows the effects of divalent cations on the thermal phase transitions of DPSG dispersions at pH 7.4. T_m of DPSG increased as the concentration of divalent cations increased. Under identical conditions, Mg^{2+} was more effective than Ca^{2+} in driving up the T_m. When 400 μM of divalent cations were added, the T_m of DPSG was approximately 63.5°C in the presence of Ca^{2+} and 67.2°C in the presence of Mg^{2+} (Table 2). Although divalent cations could increase the T_m of DPSG, the ΔH remained approximately the same over the range of the divalent cation concentrations used.

The pre-transition temperature (T_p) also increased as the concentration of divalent cations increased. Both Ca^{2+} and Mg^{2+} could increase the T_p of DPSG to approximately the same degree. When 300 μM of divalent cations were used, the T_p was 48.2 and 47.8°C in the presence of Ca^{2+} and Mg^{2+}, respectively. The pretransition of the sample in the presence of Mg^{2+} was observed in most, but not of all, samples. Its physical significance remains unclear.

Higher concentrations of divalent cations were also added to DPSG dispersions. However, sample aggregation was so great that reproducible loading of the sample into the calorimeter was technically difficult. Therefore, we have decided to use X-ray diffraction to study the effects of excess divalent cations on DASG bilayers.

X-ray diffraction of DPSG dispersions

$MgCl_2$ was added to DPSG at a three-fold molar excess. X-ray diffraction was performed at various temperatures (Fig. 5). At 20°C, DPSG existed as lamellar structures with frozen chains and a repeat spacing of 56.3 Å (Table 3). A high degree of chain order of DPSG was shown by many diffraction lines in the

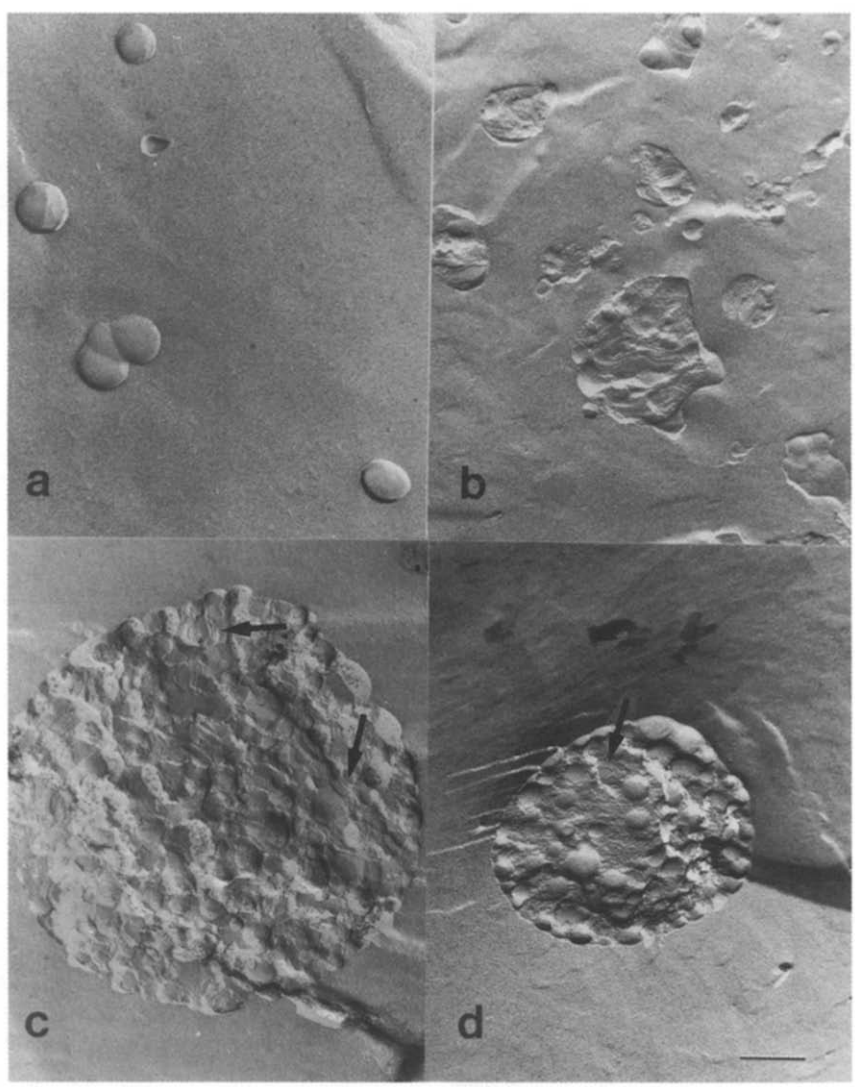

Fig. 3. Freeze-fracture electron micrographs of DOSG at (a) pH 7.4, (b) 6.0 and (c, d) 4.0. Bar = 0.2 μm.

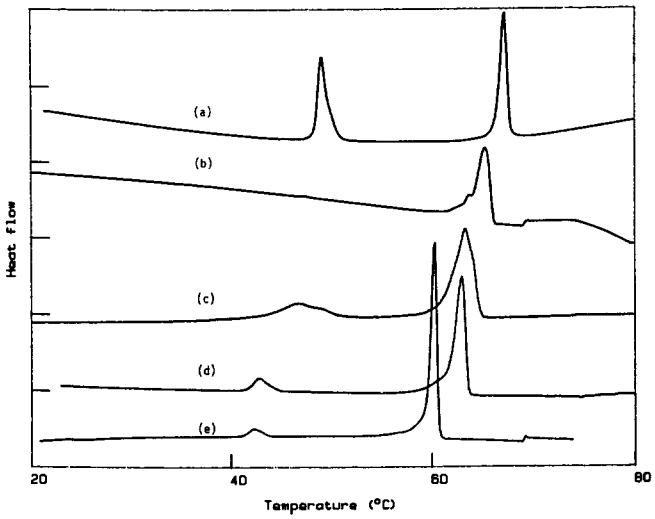

Fig. 4. Differential scanning calorimetry scans of DPSG dispersions at pH 7.4 in the presence of (a) 400 μM Mg^{2+}, (b) 200 μM Mg^{2+}, (c) 400 μM Ca^{2+}, (d) 200 μM Ca^{2+} and (e) in the absence of divalent cations.

hydrocabon chain region. Between 50–60°C, DPSG was still in a lamellar phase. However, the repeat spacing of the bilayers had increased to 61.8 Å. Also DPSG bilayers had become less crystalline as only a single, sharp diffraction line was obtained in the hydrocarbon chain region. This increase in repeat spacing is probably due to an increase in hydration. Thus, DPSG dispersions probably undergo a pre-transition at somewhere below 50°C.

At 60°C or above, DPSG dispersions underwent a lamellar to hexagonal phase transition of repeat spacing 51.8 Å and fluid or 'melted' hydrocarbon chains. Under identical conditions, the effect of Ca^{2+} on DPSG was similar to that of Mg^{2+}. The lattice repeat spacings of DPSG in the presence of Ca^{2+} at 20°C, 50°C and 70°C are shown in Table 3. The hexagonal spacing in particular is very small.

Table 2
DSC data of T_p, T_m and ΔH of DPSG dispersions in the presence of divalent cation at pH 7.4 [a]

Divalent cation [b]	μM	T_p (°C)	T_m (°C)	ΔH (kcal/mol)
Ca^{2+}	0	42.3	60.4±0.1	7.1±0.3
	100	–	61.8±0.1	6.8±0.1
	200	42.8	62.8±0.2	6.5±0.4
	300	48.2	63.5±0.1	6.8±0.2
	400	–	63.5±0.1	7.6±0.5
Mg^{2+}	0	42.3	60.4±0.1	7.1±0.3
	100	43.3	63.2±0.2	6.8±0.3
	200	46.9	65.1±0.1	6.7±0.8
	300	47.8	66.1±0.1	7.4±0.1
	400	48.8	67.2±0.1	6.4±0.5

[a] ΔH values are matched with corresponding values of T_m. Data are average values of two independent experiments ± error.
[b] Divalent cations concentrations were limiting. Molar ratio of divalent cation to DPSG < 1.

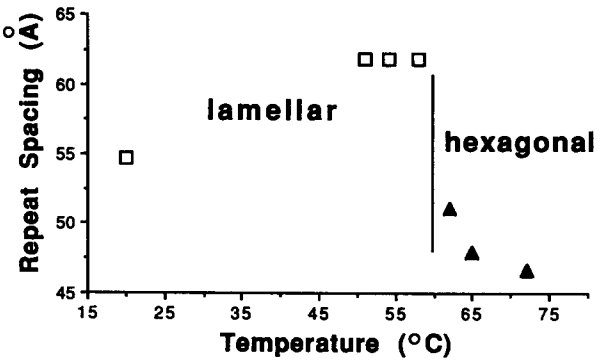

Fig. 5. X-ray diffraction measurement of the repeat spacings of DPSG bilayers in the presence of 3-fold molar excess of Mg^{2+} at various temperatures. Lamellar (□) and hexagonal (▲) repeat spacings.

DOSG dispersions with divalent cations form a hexagonal phase at 20°C. The repeat spacing of DOSG dispersions in the presence of Ca^{2+} and Mg^{2+} were similar to those of DPSG dispersions at 70°C (data not shown).

3.3. Effects of plasma on DOSG liposomes

Plasma stability of DOSG liposomes

For the use of liposomes as an in vivo drug delivery vehicle, the liposomes must be stable in the blood. We have examined the stability of DOSG liposomes in 90% normal human plasma at 37°C by measuring the release of the entrapped calcein. As shown in Fig. 6, the stability of DOSG liposomes in plasma was size-dependent. For instance after incubation in plasma for 3 h, DOSG liposomes of 256 ± 44 nm in diameter were not stable in plasma since they released 70% entrapped calcein. DOSG liposomes ranging between 126–183 nm in diameter were partially stable in plasma, releasing 30–40% entrapped calcein after incubation in plasma for 3 h. However, DOSG liposomes of 62 ± 8

Table 3
X-ray diffraction data of DPSG dispersions in the presence of divalent cations at different temperatures

Divalent cation [a]	Temperature (°C)	X-ray phase	Repeat spacing (Å)	Condition of chains
Ca^{2+}	20	lamellar	55.3	frozen – many lines
	50	lamellar	52.1	frozen – 1 line
	70	hexagonal	36.0	melted
Mg^{2+}	20	lamellar	56.3	frozen – many lines
	50	lamellar	61.8	frozen – 1 line
	70	hexagonal	51.8	melted

[a] Divalent cation concentrations were in excess. Molar ratio of divalent cation to DPSG was 3.

nm in diameter were stable in plasma, releasing only 20% entrapped calcein at the end of the 3-h plasma incubation. These data showed that DOSG liposomes that were smaller in size were more stable in plasma than DOSG liposomes that were larger in size.

Acid-sensitivity of DOSG liposomes after incubation with plasma

It has been widely documented that plasma components are found to associate with liposomes upon exposing liposomes to plasma [36]. This association may affect the acid-sensitivity of pH-sensitive liposomes, such as DOSG liposomes, after incubation with plasma.

The release of entrapped calcein, under acidic conditions, from SUV composed of DOSG before incubation with plasma was shown in Fig. 1 (closed symbol). Percent of calcein release from DOSG liposomes, prepared at various sizes ranging from 62–180 nm in diameter, was very similar to each other. After incubation with plasma, the acid-sensitivity of DOSG liposomes was reduced (Fig. 1, open symbols). The degree of reduction in acid-sensitivity of DOSG liposomes was size-dependent. For example at pH 4.5, DOSG liposomes, ranging between 126–183 nm in diameter, were found to release 70% entrapped calcein while DOSG liposomes of 62 ± 8 nm in diameter released $< 20\%$ entrapped calcein.

3.4. Cytoplasmic delivery of diphtheria toxin A chain (DTA) by the DOSG immunoliposomes

The fact that DASG vesicles undergo an acid-induced destabilization, similar to what has been observed for liposomes composed of unsaturated PE and an acidic amphiphile [16], had prompted us to examine the cytoplasmic delivery activity of DASG vesicles. DTA was used as an entrapped content marker, because it exhibits a potent inhibitory activity of protein synthesis once it gains an access to the cellular cytoplasm [37,38]. Palmitoyl anti-H2K^k was incorporated into liposome surface to enhance the binding of liposomes with the mouse L929 cells. There was a dose-dependent inhibition of protein synthesis of the L929 cells. The cellular protein synthesis in mouse L929 cells which was assayed as [^{3}H]leucine incorporation was measured as a function of the toxin concentration (Table 4). Control treatments which included empty DOSG liposomes with and without antibody, empty liposomes or immunoliposomes with free DTA added outside all showed no inhibition at the concentration range used (data not shown). The cytoplasmic delivery activity of DOSG immunoliposomes was comparable to that of the DOPE/DOSG and DOPE/DPSG (both 4:1, m/m) immunoliposomes (Table 4). We conclude that immunoliposomes composed of DOSG exhibit cytoplasmic delivery activity.

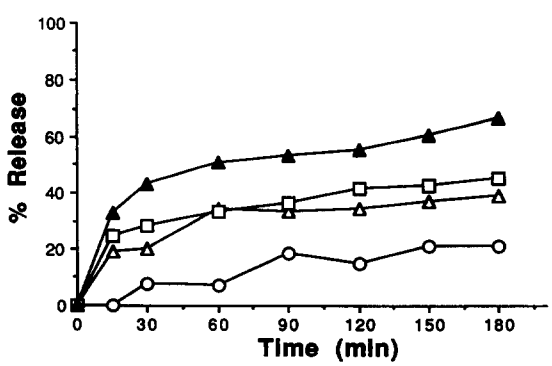

Fig. 6. Plasma stability of DOSG liposomes at 37°C. Calcein release was measured from DOSG liposomes of approximately 256 ± 44 nm (▲), 183 ± 32 nm (□), 126 ± 21 nm (▲) and 62 ± 8 nm (○) in diameter.

Table 4
Cytotoxicity of DTA entrapped in pH-sensitive immunoliposomes composed of different lipid compositions [a]

DTA concentration (mg/ml)	[^{3}H]Leucine incorporation, % control ± S.D. [b]		
	DOSG	DOPE/DOSG (8:2, m/m) [c]	DOPE/DPSG (8:2, m/m) [c]
10^{-6}	80.0± 7.9	70.9± 7.8	65.3±7.0
10^{-7}	67.2± 9.6	66.4±11.0	54.7±8.0
10^{-8}	41.0±12.1	53.4±10.0	31.5±6.8

[a] Immunoliposomes containing DTA preprared as described in Materials and methods were added to mouse L929 cells. The cytotoxicity was assayed by [^{3}H]leucine incorporation into cellular proteins.
[b] Data were expressed as ^{3}H cpm incorporation as % of control cells which did not receive any DTA.
[c] Data were taken from Ref. 16.

4. Discussion

Aqueous dispersions of both DOSG and DPSG at neutral pH had been prepared. These DOSG liposomes were found to able to entrap a H_2O-soluble fluorescent dye, calcein. While the vesicles of DOSG and DPSG are stable at pH 7.4, they undergo a rapid destabilization reaction at acidic pH. The entrapped calcein leaks out (Fig. 1). As shown by freeze fracture electron micrographs (Fig. 4B–D), DOSG vesicles were found to undergo fusion under acidic conditions.

The mechanism of acid-induced destabilization of DASG liposomes was studied with differential scanning calorimetry. DPSG dispersions showed a large endothermic ($\Delta H = 7.1$ kcal/mol), chain-melting transition at 60.4°C (Table 1). When limiting protons were present, this peak split into multiple endothermic peaks indicative of phase separation at pH ≤ 6.5 (Fig. 2). At pH 7.4, a significant portion of DPSG is already protonated. It is known that lipids in the Lα phase are more

hydrated than those in the Lβ phase [39]. Protonation of DASG would reduce the level of interfacial hydration because of the loss of the negative charge. Hence, a partially protonated DASG bilayer would be more in favor of the Lβ phase than a less protonated one. This is probably why the T_m of the main transition increases with reducing pH (Fig. 2). After a substantial fraction of DASG is protonated at even more acidic pH (pH $\leq$ 6.5), neutral, protonated species do not mix with the ionized species and phase separation occurs. But as the acidity increases, more and more DPSG becomes protonated until all the DPSG is protonated. Thus, only one predominant structure exists, for example at pH 4.6, and no phase separation can be observed. The morphology of this predominant structure had been viewed by freeze fracture electron microscopy. The structure adopted the characteristics of amorphous non-bilayer phases similar to what had been observed with α-tocopherol hemisuccinate at pH 3.5 [34].

It has been proposed that phase-separated bilayer structures are prone to fuse with each other, probably at the site of packing defects of the phase boundaries [40,41]. For example, liposomes composed of phosphatidylserine undergo rapid fusion and destabilization reactions in the presence of divalent cations which induce extensive phase separation of this acidic lipid [19,42,43].

Divalent cations also induce the destabilization of bilayers composed of DASG (Figs. 4 and 5, Tables 2 and 3). The destabilization mechanism was probably due to dehydration of the DASG bilayers. The binding of divalent cations to DASG would neutralize the negative charge of DASG and reduce the interfacial hydration of DASG bilayers, thus stabilizing the Lβ phase. This is probably why the T_m of DPSG increases as the concentration of divalent cations increases.

Mg^{2+} was more effective than Ca^{2+} in increasing the chain-melting temperature (T_m) of DPSG (Fig. 4, Table 2). Light scattering and lipid mixing experiments also showed that Mg^{2+} was more effective than Ca^{2+} in destabilizing DOSG liposomes (data not shown). This is unusual as Ca^{2+} was reported to be more effective than Mg^{2+} in destabilizing liposomes composed of anionic lipids such as phosphatidylserine [18–22] or phosphatidylglycerol [44–46]. X-ray diffraction showed that hexagonal phase structures could be observed for both Ca^{2+} and Mg^{2+} (Fig. 5, Table 3). However, at pH $\geq$ 7.4, only the formation of hexagonal phase by Ca^{2+} but not Mg^{2+} has been reported for other anionic lipids, such as phosphatidylserine, phosphatidic acid and cardiolipin [18–25].

The main structural difference between DASG and other anionic phospholipids is that DASG does not contain a phosphate group while the other anionic lipids do. The neighbouring headgroups of DASG are probably closer to each other than the neighbouring headgroups of the other anionic lipids due to the lack of repulsive force between the negatively charged phosphate groups. Mg^{2+}, being a smaller hydrated cation, may bind more effectively than Ca^{2+} to the headgroups of the DASG lipid. Alternatively, the bound Mg^{2+} ions may be more effective than the bound Ca^{2+} ions in reducing surface hydration. These nonexclusive mechanisms may explain why Mg^{2+} is more effective than Ca^{2+} in destabilizing the DASG bilayers.

pH-sensitive liposomes composed of unsaturated PE and a weakly acidic amphiphile are excellent cytoplasmic delivery vehicles [2–4,7–11,16]. We have decided to examine the cytoplasmic delivery activity of the DOSG liposomes in a manner similar to what we have previously observed for the DOPE/DASG (4 : 1, mol/mol) liposomes [16]. The data in Table 4 clearly indicated that DTA entrapped in the DOSG immunoliposomes was delivered to the L929 cells, and the observed activity was similar to that of the DOPE/DPSG and DOPE/DOSG (both 4 : 1, mol/mol) immunoliposomes (Table 4).

To use DOSG liposomes for drug delivery studies, DOSG liposomes ranging between 120–180 nm in diameter should be used. DOSG liposomes of this size are partially stable in human plasma at 37°C (Fig. 6) and retain their acid-sensitivity (Fig. 1). Since they also show cytoplasmic delivery activity (Table 4), their use in the drug delivery studies warrants further exploration.

Acknowledgement

This work was supported by NIH grants CA 24553 and AI 29893.

References

[1] Collins, D. and Huang, L. (1988) In Molecular Mechanism of Membrane Fusion (Ohki, S., Doyle. D., Flanagan, D., Hui, S.W. and Mayhew, E., eds.), pp. 149–161, Plenum, New York.
[2] Connor, J., Yatvin, M.B. and Huang, L. (1984) Proc. Natl. Acad. Sci. USA 81, 1715–1718.
[3] Ellens, H., Bentz, J. and Szoka, F.C. (1984) Biochemistry 23, 1532–1538.
[4] Duzgunes, N., Straubinger, R.M., Baldwin, P.A., Friends, D.S. and Papahadjopoulos, D. (1985) Biochemistry 24, 3091–3098.
[5] Straubinger, R.M., Hong, K., Friend, D.S. and Papahadjopoulos, D. (1983) Cell 32, 1069–1079.
[6] Huang, A., Kennel, S. and Huang, L. (1983) J. Biol. Chem. 258, 14034–14040.
[7] Collins, D. and Huang, L. (1987) Cancer Res. 47, 735–739.
[8] Connor, J. and Huang, L. (1986) Cancer Res. 46, 3431–3435.
[9] Connor, J. and Huang, L. (1985) J. Cell Biol. 101, 582–589.
[10] Wang, C.-Y. and Huang, L. (1989a) Proc. Natl. Acad. Sci. USA 84, 7851–7855.
[11] Wang, C.-Y. and Huang, L. (1989b) Biochemistry 28, 9508–9514.

[12] Cullis, P.R. and De Kruijff, B. (1979) Biochim. Biophys. Acta 559, 399–420.
[13] Liu, L. and Huang, L. (1984) Biophys. J. 24, 72a.
[14] Nayar, R. and Schroit, A. (1985) Biochemistry 24, 5967–5971.
[15] Leventis, R., Diavoco, T. and Silvius, J. (1987) Biochemistry 26, 3267–3276.
[16] Collins, D., Litzinger, D.C. and Huang, L. (1990) Biochim. Biophys. Acta 1025, 234–242.
[17] Collins, D., Maxfield, F. and Huang, L. (1989) Biochim. Biophys. Acta 987, 47–55.
[18] Newton, C., Pangborn, W., Nir, S. and Papahadjopoulos, D. (1978) Biochim. Biophys. Acta 506, 281–287.
[19] Portis, A., Newton, C., Pangborn, W. and Papahadjopoulos, D. (1979) Biochemistry 18, 780–790.
[20] Hope, M.J. and Cullis, P.R. (1980) Biochem. Biophys. Res. Commun. 92, 846–852.
[21] Wilschut, J., Duzgunes, N. and Papahadjopoulos, D. (1981) Biochemistry 20, 3126–3133.
[22] Papahadjopoulos, D., Vail, W.J., Pangborn, W.A. and Poste, G. (1976) Biochim. Biophys. Acta 448, 265–283.
[23] Rand, R.P. and Sengupta, S. (1972) Biochim. Biophys. Acta 255, 484–492.
[24] Vail, W.J. and Stollery, J.G. (1979) Biochim. Biophys. Acta 551, 74–84.
[25] Cullis, P.R., Verkleij, A.J. and Ververgaert, P.H.J.Th. (1978) Biochim. Biophys. Acta 513, 11–20.
[26] Boni, L.T., Perkins, W.R., Minchey, S.R., Bolcsak, L.E., Gruner, S.M., Cullis, P.R., Hope, M.J. and Janoff, A.S. (1990) Chem. Phys. Lipids 34, 193–203.
[27] Collins, D., Connor, J., Ting-Beall, H.P. and Huang, D. (1991) Chem. Phys. Lipids 55, 339–349.
[28] Tari, A.M., Collins, D. and Huang, L. (1990) Biophys. J. 57, 490a.
[29] Tari, A.M., Fuller, N., Rand, P. and Huang, L. (1991) Biophys. J. 59, 313a.
[30] Nicholson, G. and Blaustein, J. (1972) Biochim. Biophys. Acta 266, 543–547.
[31] Huang, A., Tsao, Y.S., Kennel, S. and Huang, L. (1982) Biochim. Biphys. Acta 716, 140–150.
[32] Gill, D.M. and Dinius, L.L. (1971) J. Biol. Chem. 246, 1485–1491.
[33] Szoka, F.C. and Papahadjopoulos, D. (1978) Proc. Natl. Acad. Sci. USA 75, 4194–4198.
[34] Ho, R.J.Y., Rouse, B. and Huang, L. (1986) Biochemistry 25, 5500–5506.
[35] Struck, D.K., Hoekstra, D. and Pagano, R.E. (1981) Biochemistry 20, 4093–4099.
[36] Juliano, R.L. and Lin, G. (1980) In Liposomes and Immunology (Baldwin, H. and Six, H.R., eds.), pp. 49–66, Elsevier, New York.
[37] Gill, D.M. and Pappenheimer, A.M. Jr. (1971) J. Biol. Chem. 246, 1492–1495.
[38] Pappenheimer, A.M. Jr. (1977) Annu. Rev. Biochem. 46, 69–94.
[39] Epand, R.M. (1990) Chem. Phys. Lipids 52, 227–230.
[40] Rand, R.P. (1981) Annu. Rev. Biophys. Bioeng. 10, 277–314.
[41] Wilschut, J., Nir, S., Scholma, J. and Hoekstra, D. (1985) Biochemistry 24, 4630–4636.
[42] Papahadjopoulos, D., Vail, W.J., Newton, C., Nir, S., Jacobson, K., Poste, G. and Lazo, R. (1977) Biochim. Biophys. Acta 465, 579–598.
[43] Wilschut, J., Duzgunes, N. and Papahadjopulos, D. (1981) Biochemistry 20, 3126–3133.
[44] Verkleij, A.J., De Kruijff, B., Ververgaert, P.H.J.Th., Tecanne, J.F. and Van Deenen, L.L.M. (1974) Biochim. Biophys. Acta 339, 432–437.
[45] Ververgaert, P.H.J.Th., Verkleij, A.J. and Van Deenen, L.L.M. (1974) Chem. Phys. Lipids 12, 201–219.
[46] Van Dijck, P.W.M., Ververgaert, P.H.J.Th., Verkleij, A.J., Van Deenen, L.L.M. and De Gier, J. (1975) Biochim. Biophys. Acta 406, 465–478.